SmallSat Alliance Collegiate Space Competition: Orbital Debris

BROOM (Bio-friendly Recycling Operation of Orbital Material) Mission

Aubrey Baker
Diana Segura Lerma
Madison Vaughan
Mauricio Martinez Elizondo

Seniors in Aerospace Engineering Undergraduate Program
The University of Texas at Austin

With thanks to Adam Nokes, Karim Emara, Keith Todd, Dr. Scott Dorrington, and Ben Clark

Executive Summary

The SmallSat Alliance (SSA) is sponsoring a national competition that aims to motivate students to develop innovative technical and policy solutions to modern-day challenges by taking advantage of the agile capabilities of small satellites. The mission described in this paper is a proposed solution to the challenge posed by the SSA to "propose a realistic and environmentally safe solution to dispose of old rocket and satellite debris."

To solve the challenge proposed by the SSA, the proposed design aims to provide an alternative approach to many Active Debris Removal (ADR) missions. Instead of deorbiting a single piece of debris to burn up during re-entry, this proposal describes a mission that collects multiple space debris objects in an aggregation orbit. In this way, the mission is capable of removing multiple debris objects, while also avoiding the environmental hazards of deorbiting and providing an innovative approach that leads to a future of in-space manufacturing and space resource recycling.

This proposal provides a detailed concept of operations of the BROOM (Bio-friendly Recycling Operation of Orbital Material) mission. Furthermore, an extensive literature review of past debris removal missions and academic research projects that have influenced the mission design is shown. In addition, this document provides in-depth analysis of the debris target selection process. Novel design approaches for capturing mechanisms are described in the body of the design paper. This includes the design of two satellites: the Collection Satellite and the Aggregation Satellite. Further details of the mission, such as the spacecraft mass budget and the propulsion system, are included in the design submission.

Table of Contents

Executive Summary 2
List of Abbreviations 4
1 Problem Statement 5
2 Background 5
3 Literature Review 7
3.1 Target Selection 7
3.2 Propulsion 11
3.3 Capture Mechanism 13
3.3.1 Claw 14
3.3.2 Bag 16
3.4 Electropermanent Holding Magnet 17
3.5 Deployable Composite Booms 20
4 Approach to the Design Challenge 22
4.1 Concept of Operations 22
4.1.1 Satellites 22
4.1.2 Mission Phases 22
4.2 Target Selection 24
4.2.1 Collection Orbit 24
4.2.2 Aggregation Orbit 26
4.2.3 Tracking Algorithm 28
4.3 Collection Satellite 31
4.3.1 Claw 31
4.3.2 Bag 32
4.3.3 Dispenser 32
4.4 Aggregation Satellite 33
4.4.1 Bag Holding Mechanism 33
4.4.2 Deployable Boom 34
4.4.3 Final Aggregation Satellite Design 34
4.5 Propulsion 35
4.6 Mass Budget 37
5 Scale-Up of Design Approach 38
6 Implications of Design Approach 39
Appendix A: Contact Information 40
Appendix B: University and Program Description 41
Appendix C: Industry Expert Description 42
Appendix D: Educational Experience 43
Appendix E: References 46

List of Abbreviations

Abbreviation	Definition
ADR	Active Debris Removal
BHT	Busek Hall Thruster
BROOM	Bio-friendly Recycling Operation of Orbital Material
DCB	Deployable Composite Boom
GEO	Geostationary Orbit
HET	Hall-Effect Thruster
IDO	Intact Derelict Object
ISS	International Space Station
LEO	Low Earth Orbit
MLI	Multi-Layer Insulation
SMAP	Soil Moisture Active Passive
SSA	Small Satellite Alliance
TLE	Two-Line Element

1 Problem Statement

Space debris generated by defunct satellites, inert rocket stages, and particle debris as the result of space collisions pose an ever-growing threat to the commercial and private space industry. Hypervelocity impacts of such debris increase the risks of all spacecraft missions. This proposal proposes a realistic and environmentally safe solution to dispose of old rocket and satellite debris.

2 Background

When trying to define the term, “environmentally safe” in relation to orbital debris disposal, it is important to first look at the effect deorbiting has on Earth’s atmosphere. Deorbiting is a typical operation for satellite, rocket, and debris disposal, where the spacecraft re-enters at a specific angle to maximize the burn of its material. Deorbiting is essentially the equivalent of burning one’s trash instead of putting it in a landfill. Most defunct satellites that deorbit at the end of their lifespans will burn and release possible pollutants. This method of satellite disposal was common in a time when there wasn't exponential growth of commercial satellite-based technology, so in the grand scheme of things, what did it matter if some hundred satellites ended up burning up over the years? Furthermore, until 1978, when Don Kessler and Burton Cour-Palais published a prediction about the growing dangers of debris being created by collisions alone, there weren’t any programs or organizations dedicated to the debris problem [1]. This meant that awareness about the growing problem and possible risks to missions did not garner attention until that point. Even after the concept of the Kessler Syndrome was published, it is likely that the future implications of the debris problem were understated due to there being fewer satellites active at that time and debris-based collisions not being very common.

Yet 50 years later, the state of the space commons is growing at a faster rate than ever seen before. That means more deorbiting, collisions, and risk to astronauts and people on Earth. There might not be an environmental crisis due to this satellite debris yet, but it's certainly easy to rationalize in the future. In the last decade, studies have shown a 60% increase in orbital debris, especially following the Chinese Fengyun-IC destruction test in 2007 and the Iridium-33 and Cosmo 2251 collision in 2009 [2]. Those two events alone contributed to a sharp increase in total objects in orbit around the Earth, as seen in Figure 1.

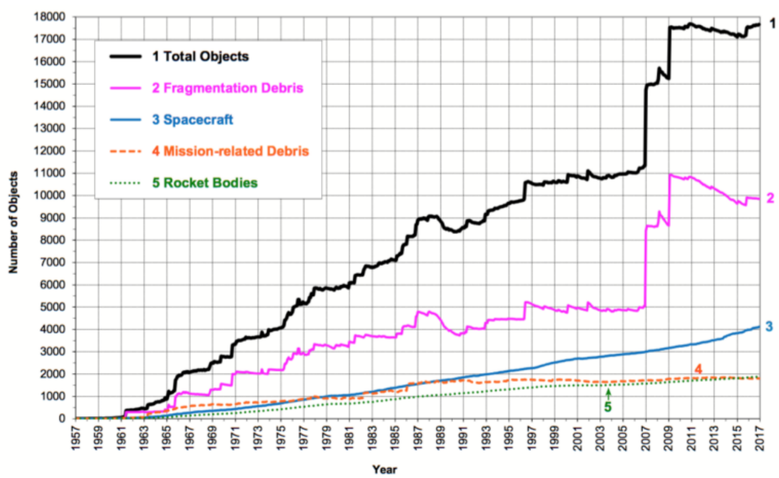

Figure 1: Monthly number of object in Earth orbit by object type [3]

Evidently, the guidelines by the FCC to let a defunct satellite 'sit and wait' to deorbit itself under 25 years (and as of September 2022, under 5 years) will only further contribute to this growing problem. For this reason, the definition of an "environmentally safe" mission is one that does not result in the deorbiting of debris. Instead, the mission solution will be working toward the greater goal of aggregating pieces of debris to create an easily trackable and accessible 'scrapyard' of defunct satellites that can eventually be taken apart and recycled. The long-term vision is that these collected parts could be used for growing On-Orbit Servicing, Assembly, and Manufacturing (OSAM) missions. This concept of recycling satellite debris is especially exciting as technology in general is morphing to encompass more sustainable practices, but the details of how this would work are outside of this proposal's scope. Instead, this mission focuses on the collection and aggregation of debris in the regions of LEO that are most densely populated and simply acknowledges the potential for continuation of this vision in the future.

3 Literature Review

3.1 Target Selection

Research has been done to classify space debris objects to help make decisions on active debris removal (ADR) target selection [4].

Characteristic	LNT – Lethal Nontrackable Debris		CF – Cataloged Fragments		IDO – Intact Derelict Objects (R/Bs and Nonoperational P/Ls)	
	LEO	GEO	LEO	GEO	LEO	GEO
Mass Range	1 gm – 500 gm	500 gm - 10 kg	500 gm - 10 kg	10 – 15 kg	>10 kg	>100 kg
Size Range	5 mm – 10 cm	10 cm - 1m	10 cm – 1 m	1 m - 2 m	>1 m	>2 m
Total Number	–600,000	–2,000	–8,100	–1,000	–2,500	–620
Total Mass	–100 kg	–1,000 kg	–100,000kg	–10,000 kg	–2,000,000 kg	–1,000,000 kg
Average Relative Impact Velocity	10 km/s	200 m/s	10 km/s	200 m/s	10 km/s	200 m/s
Effect of Impact on Large Object	Mission-degrading or mission-terminating		Mission-terminating and debris production		Significant debris production	
LNT Produced	N/A		–10 /kg	–2 /kg	–50 /kg	–10 /kg
CF Produced			N/A		–10 /kg	–2 /kg
Characterization Issues	Cannot detect or track regularly from the ground		Mass, shape, and density difficult to determine from size		Tumble rate is unclear but dry mass is well known	
Distribution In Orbit	Assume to be distributed in altitude and inclination similarly to CF and IDO		Contours follow previous breakup events and quantified by the satellite catalog		Contours follow popular orbits	
	Affected significantly by drag	Affected significantly by solar radiation pressure	Below 950 km debris is very populous	Some fragments will migrate to gravitational wells	Depends on deployment process – several major clusters of concern	Most derelicts will oscillate about gravitational wells
Removal Issues	Requires large surface area collector with a robust structure capable of maneuver		Requires large surface area collector that is durable and capable of maneuver		May be tumbling, hard to grapple, and require system to move; LEO to deorbit but for GEO move to graveyard orbit	

Figure 2: Three families of debris for possible ADR targets [4]

Detailed analysis has shown that the removal of bigger and more massive objects would constitute a higher impact than the removal of smaller objects. This makes the Intact Derelict Objects (IDO) category the most desirable for target selection. However, extremely big objects pose added complications, such as a higher mass required from the spacecraft performing the removal. Therefore, missions can be planned by aiming to target the biggest objects possible with the available mass for each specific spacecraft.

Furthermore, analysis has been done on the altitudes, inclinations, and other orbital parameters with the highest density of objects.

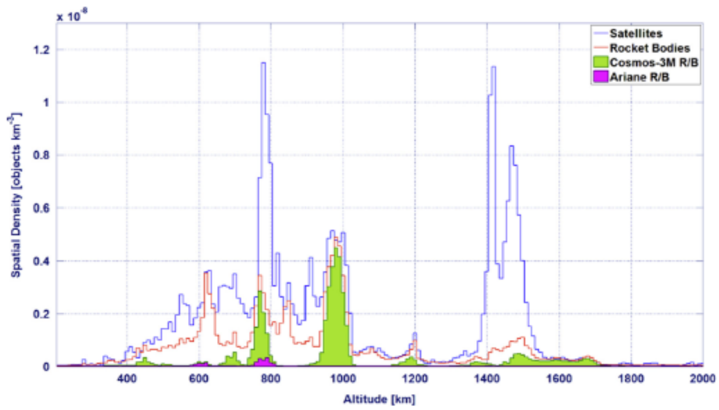

Figure 3: Spatial density per orbit altitude [5]

There are clear peaks of objects in the 800-850 kilometers range of altitude, as well as between 1400-1500 kilometers. However, the 800-850 kilometer region has been the place for more catastrophic debris events with new communications satellites.

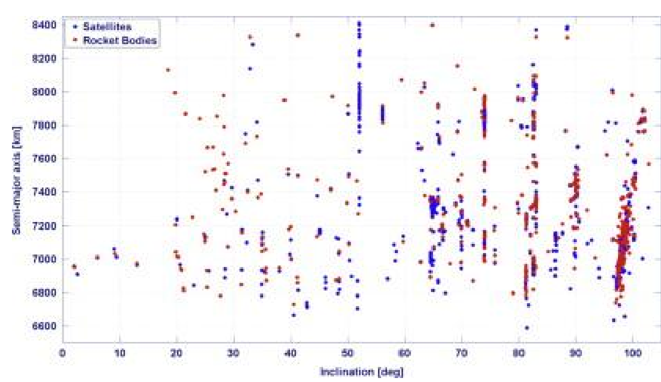

Figure 4: Density of objects per semimajor axis and inclination [5]

Furthermore, the inclination plot points us to the idea that the 90°-100° degree inclination region is the most congested one, indicating it is the best one for ADR targeting.

The mission aims to perform multiple maneuvers of placing the target debris object in a higher orbit. Therefore, it is necessary to develop an optimal method to approach different objects depending on the delta-v budget of the spacecraft and the multiple physical characteristics that might lead to a desirable debris object for capturing.

Solutions to this problem are scarce in the available literature. Most of the conceptualized ADR missions have focused on approaching one specific object of interest instead of aiming to capture multiple objects by performing a mission with multiple maneuvers from the target orbit to a depot/collection orbit.

Due to the uniqueness of the BROOM mission concept, a novel method to determine the optimal target debris objects was conceptualized. To do this, multiple graph theory solutions were compared to find the best option to solve a type of orbital target optimization problem.

For the Knapsack Problem, a set of N nodes (items) is considered, each with a defined score and weight. A subset of items is determined to select that maximizes the total score, subject to a constraint on the total weight. This method can be applied to satellites to model the problem of out-and-back trips from a depot to individual satellites. For this, it is assumed that each trip is independent of previous trips. Then, selecting which satellites to visit is the problem to solve. For this implementation, items are individual satellites. Each satellite has a score, dependent on physical characteristics, such as mass or Radar Cross Section. Weights define the out-and-back delta-V or distance to visit the satellite and return.

For the Orienteering Problem, a set of N nodes is considered, each with a defined score, and a set of distances between each pair of nodes. A tour that starts and ends from a specified node that maximizes the total score is found, subject to a constraint on the total path length. This problem can be applied to satellites to model the problem of departing from a depot, visiting a subset of satellites, and returning to the depot. As before, nodes are individual satellites. Each satellite has a position (orbital parameters), and a score (dependent on physical characteristics). Distances between satellites are defined by delta-Vs or other distance metrics.

One example of an optimization solution applied to an ADR mission is shown in a paper by Federici, Zavoli, and Colasurdo. They apply a method of A* search for mission planning. This is similar to a time-dependent orienteering problem [6]. In their implementation, they focus on a cluster of debris orbiting the sun-synchronous orbit. A numerical score is given to each debris based on level of threat. Their goal is to maximize the cumulative score of the removed debris by meeting requirements of delta-v and mission time. The implementation requires an optimal tree search algorithm. To fulfill the delta-v requirement, delta-vs are pre calculated with a near-optimal transfer strategy.

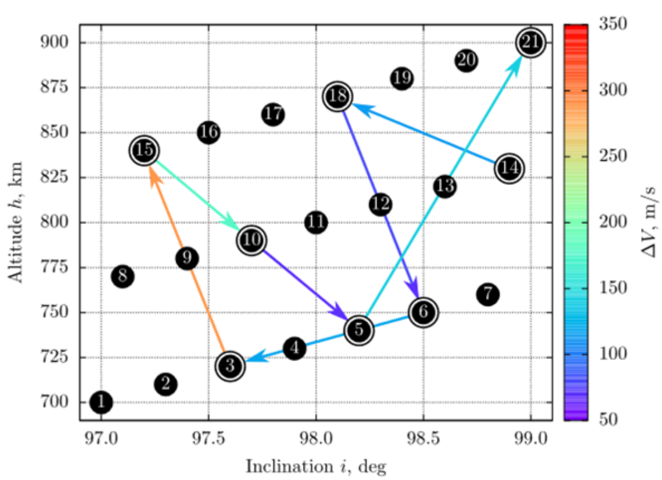

Figure 5: Optimal removal sequence [6]

The literature review shows that previous implementations use delta-V as a distance between nodes. This requires an extensive numerical computation depending on the accuracy of the method used to calculate delta-v.

3.2 Propulsion

In order to select an Electrical Propulsion system for this mission that used Xenon as propellant, many sources were investigated. The parameters for the only EP systems with flight heritage as of 1999 are described in Table 1.

Thruster	Specific Impulse (s)	Input Power (kW)	Efficiency Range (%)	Propellant
Cold gas	50–75	—	—	Various
Chemical (monopropellant)	150–225	—	—	N_2H_4 H_2O_2
Chemical (bipropellant)	300–450	—	—	Various
Resistojet	300	0.5–1	65–90	N_2H_4 monoprop
Arcjet	500–600	0.9–2.2	25–45	N_2H_4 monoprop
Ion thruster	2500–3600	0.4–4.3	40–80	Xenon
Hall thrusters	1500–2000	1.5–4.5	35–60	Xenon
PPTs	850–1200	<0.2	7–13	Teflon

Figure 6: Nominal operating parameters for thrusters with flight heritage [7]

The only two options to select the mission's thrusters came down to Ion thrusters and Hall Effect Thrusters (HET) since they are the only ones with flight heritage dating back over twenty years, and they are the ones most widely used today. Because the mission itself is very experimental, the longevity of mission heritage was prioritized. [8]

However, according to a NASA publication of State-Of-the-Art in-space propulsion, Hall Effect thrusters are “the most successful in-space EP technology.” [9] Following this recommendation, the only thing left to do was select the specific HET. In this same paper, NASA mentions BHT (Busek Hall Thruster) over 15 times because there is a substantial amount of mission heritage, research, and testing performed by NASA for the use of Busek’s thrusters.

Given the overwhelming mission heritage and tests presented in this publication for the BHT, it was decided that a Xenon EP thruster from Busek was to be selected for the mission. From the many BHT Xenon EP thrusters available, the one selected was the BHT-600 with TRL of 5 or above as of 2019. [10] The BHT-600 thruster specifications are listed below:

Parameter	Value
Disharge Potential	300 V
Discharge Current	2.0 A
Discharge Power	600 W
Thrust (Xenon)	39 mN
Specific Impulse (Xenon)	1495 s
Lifetime (Demonstrated)	>5,000 h
Througput (Demonstrated)	>48 kg
Total Impulse (Demonstrated)	>700 kN-s

Figure 7: BHT-600 nominal specifications [11]

The BHT-600 thrusters were selected because they were specifically optimized for small spacecraft with high delta-v missions, and it has an ISP of 1500s which is sufficient to "lift a 140 kg spacecraft from LEO to GEO, including a 28-degree inclination change – a maneuver which requires a total delta V of approximately 6.0 km/s". The satellite will be equipped with two BHT-600 for precaution and to aid in maneuverability. This number can be increased at a later point after a power budget is performed to ensure the mission has the capacity to operate more than two thrusters at a time [11].

It is also important to mention that this same thruster was presented in NASA's previously mentioned State-Of-the-Art in-space propulsion publication, describing a successful 7,000-hour ground test of the system [9]. The paper presenting an overview of Busek's EP systems also presented the results and discussion for the same ground test [11].

3.3 Capture Mechanism

The researched capture mechanisms include a net, claw, and harpoon. The net captures debris by using a deployable net with a diameter of 5 m, which can capture debris up to 12 m in size and handle up to 8 tonnes [12]. The net must be within 7 m of the target [13]. The net is designed to deorbit the target and burn up in the atmosphere, making it an environmentally safe option. The net's accuracy is guaranteed by increasing its size to ensure capture.

The claw mechanism, such as ClearSpace-1's claw configuration, can capture debris up to 112 kg [14]. The claw moves slowly and steadily to ensure proper disposal of the captured debris, making it environmentally safe. The claw's accuracy is 100% because the claw has physical contact with the targeted debris, enveloping it securely. The claw can be made of either light composite or heavy structural material, depending on the required mass. The claw has been tested in previous missions. ESA's ClearSpace-1 claw was able to successfully rendezvous with a tumbling target and secure the target within the claw mechanism [15]. This shows that even though the GNC capabilities of this mechanism are extremely advanced, it is possible to approach, capture, and secure a piece of debris– let alone a piece of tumbling debris.

The harpoon mechanism pierces the targeted debris and captures it. A harpoon weighs around 8kg, with an additional 1.3 kg for each extra harpoon [16]. While the harpoon mechanism can capture unlimited debris up to 9000 kg, it has the potential to cause more orbital debris upon the piercing of the targeted debris [16]. The harpoon mechanism's accuracy is less than 5 cm at 10 m distance from the target [16]. Even though this mechanism appears to be able to accomplish many of the tasks that the mission will need to carry out, the obvious downfall of this solution is the inevitable effect of piercing the debris. Upon piercing the debris, an excess of debris will be created which goes against exactly what this mission is trying to accomplish. While this solution may not satisfy this particular mission's needs, it has been proven successful in a demonstration mission called RemoveDEBRIS [17].

While each capture mechanism has its advantages and disadvantages, the claw mechanism appears to be the most environmentally safe and accurate method of capturing debris, with a large capture size and the ability to ensure proper disposal. The net mechanism is also environmentally safe and accurate but may require a larger net to capture larger debris. The harpoon mechanism has the potential to cause more debris thus does not resolve the growing orbital debris issue at hand.

3.3.1 Claw

Robotic arms are an essential tool for space exploration and have been used extensively in a wide range of space missions. These arms are typically designed to be highly versatile and capable of performing a wide range of tasks, including deploying and retrieving payloads, and conducting maintenance and repairs on satellites and other space-based assets.

For this application, the claw will be required to take out a debris bag from the bag dispenser within the satellite, position a debris bag properly within the claw, close the bag once debris captured within the bag, and transfer the bag from the collector satellite to the aggregator satellite with the mag-lock boom system. These tasks require a robotic arm with multiple digits.

The claw design is inspired by robotic arms that have been used in past and present missions. The robotic arms that this section looks into are the Canadarm 2, European Robotic Arm, ClearSpace-1, and the arm deployed on the Soil Moisture Active Passive (SMAP). For the material composition of the robotic arm the Canadarm 2, European Robotic Arm, and SMAP arms are investigated. The ClearSpace-1 robotic arm was used as a reference for sizing.

The primary purpose of the Canadarm2 is to provide a means of moving equipment and supplies, as well as to assist astronauts during spacewalks. It has seven motorized joints, allowing it to move and position objects with great precision [18]. It also has a unique end effector, which is capable of grasping and manipulating objects of various shapes and sizes.

The European Robotic Arm was installed on the International Space Station (ISS) to assist with maintenance and check-ups on the ISS. It has four motorized joints and an accuracy of 5 mm [19], and it has infrared cameras to help assist these checkups and observations.

The SMAP robotic arm does not have any dexterity but rather extends to deploy a reflection dish [20]. While the application is not the same, the robotic arm materials and joints are of interest for the design of the orbital debris mission.

The use of the robotic arm on the orbital debris mission does not need the same type of accuracy nor technical aspects as those missions described above. Instead, the aspects that are considered when designing the robotic arm are the conditions that these robotic arms operate in. The Canadarm 2, European Robotic Arm, and SMAP arms are made out of carbon reinforced plastic [18] [21] [20]. This material has a lot less mass in comparison to traditional materials known for strength such as steel and aluminum. More specifically, the carbon fiber reinforced plastic is found to have 50% less mass than aluminum and 20% less mass than steel [18]. This is beneficial for the orbital debris mission as the mass requirements need to remain under 180 kg for the entire small satellite.

The ClearSpace-1 mission was used as a reference for sizing. The ClearSpace-1 mission's aim is to contribute actively to cleaning up space through the use of a claw mechanism much like the one this orbital debris mission uses. In addition, the working conditions of the ClearSpace-1 mission is comparable to the parameters of this orbital debris mission – low earth orbit, targeting space debris, and utilizes a claw. As such, the measurements of the robotic arm on the orbital debris mission are scaled from the ClearSpace-1 mission. More specifically, the ClearSpace-1 mission was targeting a piece of debris that had a 2.18 m diameter and height of 2.04 m [22].

3.3.2 Bag

As described previously in this paper, the orbital debris will be contained within a bag. This section details the trade study between Mylar (multi-layer insulation - MLI) and Beta cloth Mylar and beta cloth are two materials that have different properties and general uses. As such, they are used for a wide range of engineering applications. Mylar is a type of polyester film that is known for its flexibility, strength, and versatility. It is commonly used in packaging, insulation, and as a reflective coating. Mylar is a highly reflective material that is often used in space blankets to help keep astronauts warm. It is also used in solar sails, which are large, lightweight structures that harness the energy of the sun to propel spacecraft through space.

Beta cloth is a high-strength woven fabric that was originally developed for the Apollo space program in the 1960s. It is made from a combination of Teflon-coated fiberglass and beta-fiber yarns, which gives it exceptional strength, durability, and resistance to heat and abrasion. Beta cloth is used in spacesuits because it can withstand the extreme conditions of space, including high radiation levels and micrometeoroids.

More specifically, the material properties that contribute to Mylar's unique abilities are the density, tensile strength, and thickness. The density of Mylar is 1.39 g/cm^3[23] . The tensile strength is reported in psi – different from beta cloth. Mylar has been tested and is shown to have a tensile strength of 28,000 psi in the axial direction and 34,000 psi in the transverse direction [23]. Considering that the bags will be stored within the collector satellite, the bags need to fold up neatly and compactly. From the CS Hyde catalog website, the thickness of available-to-purchase Mylar can range from 0.025 cm to 0.127 cm.

Beta cloth has different material properties than Mylar, yet it is still a contender for the material of the orbital debris bag. Beta cloth has a density of 7.6 g ms [24]. In addition, the tensile strength of beta cloth is greater than 80 lb in [24]. The tensile strength is reported in lb/in – different from Mylar. The difference stems from the fact that beta cloth is made of fibers. Fibrous materials measure the tensile strength in force per fiber. To put the tensile strength of beta cloth into perspective, a generic cotton thread size 35 has a tensile strength of about 2 lb in [25]. For a material of this strength and density, one would imagine that the material would be thick and cumbersome. However, the thickness is 0.008 inches [24].

Other considerations of the material capabilities when designing the orbital debris bag include cost, accessibility, and recyclability. Part of this design mission is to propose a realistic solution to dispose of old rocket and satellite debris. In order for the mission to be realistic, the cost of the components needs to be practical. Luckily, the multi-layer insulation is widely available for purchase for anyone. A roll of Mylar is currently $250.60 in the CS Hyde Company catalog with the following specifications: 0.010" thick Metalized Polyester PET film 40" wide roll x 25' [23]. This indicates that each square foot of Mylar is about $4.00 per square foot of material. Unfortunately, beta cloth is not a widely available material. Beta cloth was developed by NASA and is mainly used for space application. Since its use is so limited, the material is not commonly found nor are the specifications. Consequently, the cost for this material is unknown.

3.4 Electropermanent Holding Magnet

An empirical study was done by Cornell University to observe the application of passive magnetic methods for close proximity spacecraft operations [26]. The study outlines a proof-of-concept for using electropermanent magnets as failure-tolerant docking mechanisms between a satellite and a robotic arm end effector in different rendezvous scenarios.

The concept of rendezvous and magnetic docking between a satellite and an end effector is especially relevant to the aggregation satellite, as the bag of debris captured by the collector satellite will be ‘docking’ to extremities on the aggregation satellite. The intent is that the aggregation satellite will remain as passive as possible, requiring little mechanisms outside of deploying its extremities and solar arrays, and controlling its communication and power systems, thus a passive and simple docking mechanism is of interest for this design. However, there still needs to be some element of control to activate the system, as past studies into completely passive magnetic docking have shown the need of an attitude control system due to the uncontrollable magnetic torques exerted on the spacecraft [26].

Electromagnets are a compelling solution because the magnetic field is controllable by actuating the power supply, and they have heritage in aerospace applications. However, to maintain the magnetic field, the electromagnet must receive a constant supply of power for however long the latching is desired, introducing a level of risk to the mission should power systems fail or unexpectedly turn off [26]. The risk of collected debris disconnecting from the aggregation satellite would be too likely, and another solution must be found.

Electropermanent magnets combine the electromagnet’s ability to actuate the magnetic field due to power supply and the permanent magnet’s ability to be failure-tolerant in a passive state. An electropermanent magnet consists of one hard and one soft rare earth magnet, placed next to each other with electromagnetic ‘switching’ coils wrapped around them. Turning the coils on magnetizes the soft earth magnet and increases the permanent external magnetic field created even after the coils have been turned off.

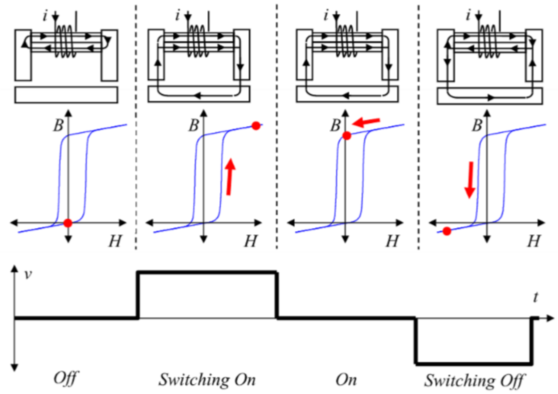

Figure 8: Switching Effects on Electropermanent Magnet [27]

This study identifies these magnets as a passive mechanism that is best suited for safe, fail-tolerant docking. The study then conducts experiments using different rendezvous scenarios between the end effector electromagnet and a mock satellite, where the magnet's coils were switched on at different points in the approach in order to see which scenario resulted in the greatest external magnetic field. The experiment found that the holding force was greatly improved when the coils were switched on after physical contact with the target was already made, and that previous activation of the coils did not negatively affect the holding force [26].

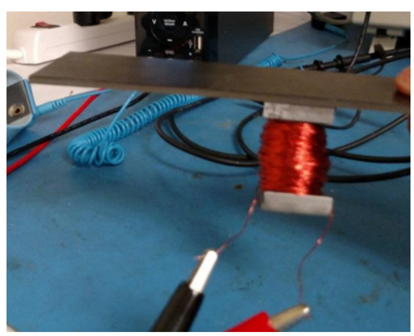

Figure 9: Electropermanent magnet attached to ferrous plate [26]

These results show a proof-of-concept for using electropermanent magnetic docking between the collection bag and aggregation satellite, where the bags could attach to an electropermanent magnetic receiver along the extremities of the satellite by making physical contact between a ferrous plate on the bag and having the receiver switch on for a short period of time. More bags could be added in a series with multiple of these magnets being activated simultaneously without the risk of previous bags unlatching from their magnetic hold. This proof-of-concept shows confidence in the technology, thus it was selected for a portion of the design for the aggregation satellite.

3.5 Deployable Composite Booms

NASA has been recently developing lightweight, foldable, Deployable Composite Booms (DCBs) at the Langley Research Center in Virginia. DCBs are made to unroll from a motorized spool into a rigid, carbon fiber tube that could extend several meters from the main body of a satellite. The tube is created in a unique shape, where it can both lay completely flat within the spool but also pop open automatically as the spool unrolls.

Figure 10: DCB unrolling from spool [28]

One design places four of these booms co-wrapped onto one spool, where the single motor will unroll the four booms at once in the four separate directions to form the structure of the solar sail [28]. The quad-directional deployment mechanism has been proven to work in a laboratory setting and thus is a compelling new piece of technology that could be utilized for this mission, and because of the simple design of a single-motor actuation, there is great reliability in the deployment.

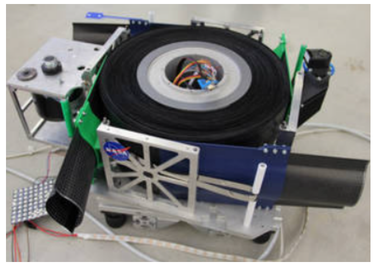

Figure 11: Co-Wrapped DCB spool [28]

One mission at the Langley Research Center is utilizing a modified version of this design, named the Advanced Composite Solar Sail System (ACS3), designed to use a 12U CubeSat structure. The ACS3 mission utilizes 4 separate spools for each boom, instead of the previously discussed co-wrapped spools. This indicates the scalability of this technology, where concepts could be combined to fit the bus size of the aggregation satellite

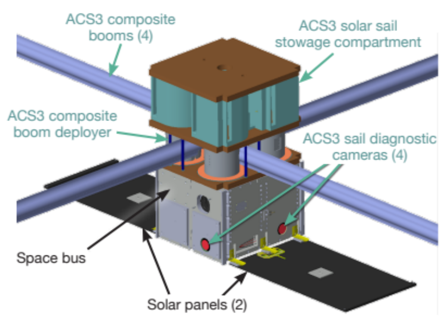

Figure 12: The ACS3 DCB design [29]

The benefit of DCBs is also the potential to store internal components, such as wires, along their internal structure. For the aggregation satellite, electropermanent magnets and their respective wiring was integrated into the booms, it should be realistic to have a relatively simple deployable extremity to which the collection satellite could attach bags. For this reason, this technology was chosen for a portion of the aggregation satellite design.

4 Approach to the Design Challenge

4.1 Concept of Operations

4.1.1 Satellites

The Collection Satellite is a SmallSat with a dry mass of up to 180 kg and a wet mass of up to 500 kg. It will be launched along with the aggregation satellite using the same launch vehicle and opportunity to go to space. However, it will be deployed at a lower altitude of 850km in the same inclination. The collection satellite is equipped with a deployable robotic arm/claw and an empty debris bag. The robotic arm/claw can grab debris up to $1m^3$ in size. The debris bag is made of a material that can accommodate and encapsule the debris collected.

The aggregation satellite is a 6U CubeSat with a maximum dry mass of 12kg. It will also be launched using the same launch vehicle and opportunity as the collection satellite, but it will be deployed at a higher altitude of 1300km in the same inclination. The aggregator satellite is equipped with deployable booms that are capable of holding debris bags. The booms can each hold up to 20 debris bags at a time.

4.1.2 Mission Phases

Phase 1 - Launch: The collection satellite and the aggregator satellite will be launched together using the same launch vehicle and opportunity to go to space.

Phase 2 - Deployment: The collection satellite will be deployed at an altitude of 850km, while the aggregator satellite will be deployed at an altitude of 1300km. During the deployment phase, both satellites will undergo detumble, initial, and payload checkout. These subphases ensure that both satellites are functioning correctly before the remaining operations begin.

Phase 3 - Collection: The collection satellite will use its robotic arm/claw to grasp the debris and place it inside the debris bag.

Phase 4 - Delivery: Once the debris bag is full, the collection satellite will perform a series of thruster burns to boost its orbit to 1300 km to deliver the debris bag to the aggregation satellite. Once the Collection Satellite is in close proximity to the aggregation satellite, the spacecraft's robotic arm/claw will attach the bag to the aggregation Satellite's booms. The closing of the bag will dock with a Maglock station on the boom which will activate when the mating is confirmed. The Maglock will then deactivate by the stop of current and the bag will hang from the boom permanently. The transfer process will be monitored and controlled from the ground to ensure its success. Eventually, this process should be automated.

Phase 5 - Repeat: Once the delivery phase is complete, the collection satellite will return to its original altitude of 850km in order to start collecting debris again.

Phase 8 - End-of-life: The mission is estimated to last five years. After these five years, the aggregation satellite will attach itself to a Maglock station and will then be considered debris as well. This will conclude the mission. However, as mentioned before, the long-term goal is for a third-party agency to pick the aggregation satellite up to make use of the parts in order to avoid wasting those materials by deorbiting the aggregation satellite and burning up upon atmospheric re-entry.

Descope: In the long-term event that the aggregation satellite cannot be collected to sort through and reuse or recycle the materials, a ConOps descope would occur. The aggregation satellite will be equipped with terminator tape in order for it to deploy it, lose altitude, and burn upon re-entry in a worst-case scenario. This would not affect mission success.

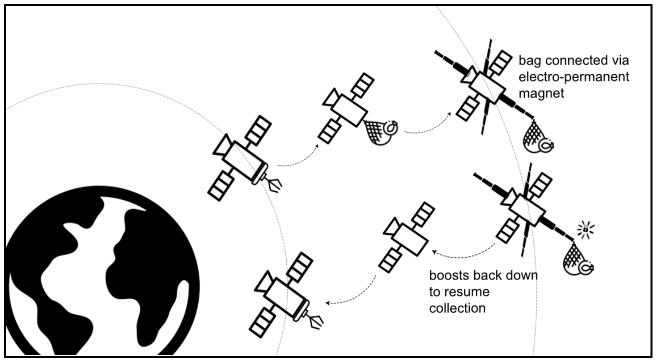

Figure 13: Complete concept of operations diagram

4.2 Target Selection

4.2.1 Collection Orbit

To perform initial debris target selection, the general space debris population will be studied. From this analysis, a specific altitude and inclination will be chosen as the initial target for the mission. To begin the analysis, distribution of objects in Low Earth Orbit (0 km - 2000 km) was plotted. However, to be more specific for the mission, the object database was filtered.

The first step was to obtain the space object catalog. The Spacetrack dataset (from space-track.org) provides an online open-source database of the orbital parameters of the space object catalog tracked by the USSPACECOM. The database's API allows users to query the database and obtain Two-Line Elements (TLEs) for each space object. From this, a dataset for all space objects tracked by the USSPACECOM with their respective characteristics can be obtained. Aside from Keplerian orbital elements and angular momentum coordinates, some examples of the characteristics that can be accessed are Dry Mass, Country of Origin, Radar Cross Section, and Object Type. For the purposes of the mission, the database is filtered by the semimajor axis/altitude (only using LEO objects), by country (only using objects owned by US, Japan, or France), and by object type (only using debris objects/rocket bodies). After filtering the dataset, a plot of altitude vs. inclination is obtained.

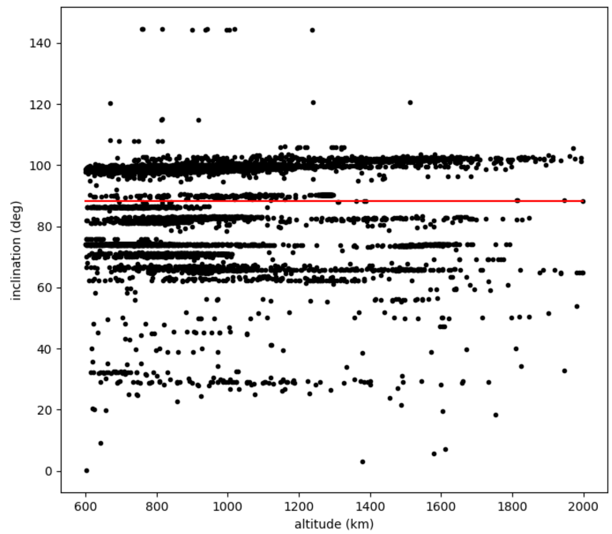

Figure 14: Distribution of objects in LEO for altitude and inclination

A clear trend can be seen in this plot, which aligns in principle with the research covered in the background section. There seems to be a congested region around 100 degrees of inclination and 800-850 km of altitude. To begin, the altitude of the database can be further restricted to be between 800 - 850 km.

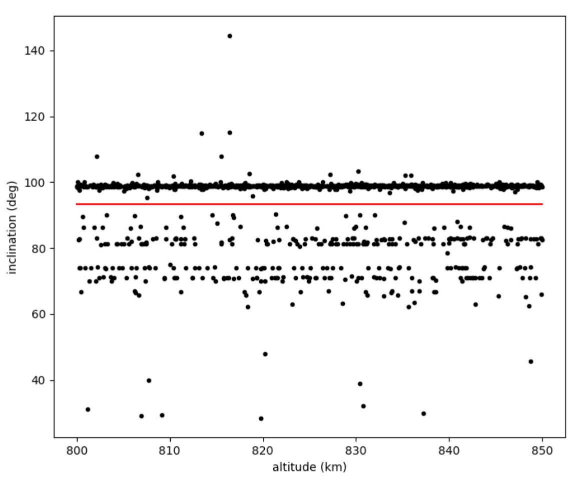

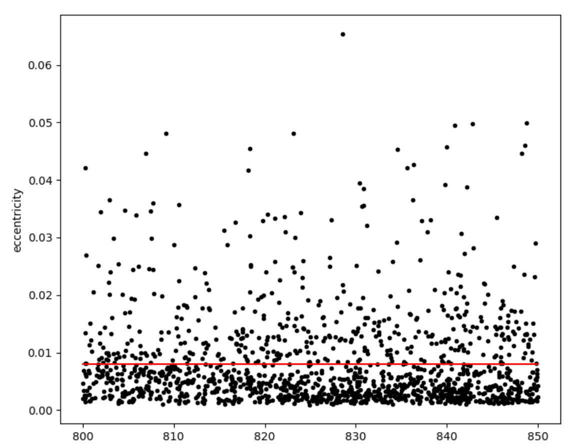

Figure 15: Objects inclination 800 - 850 km altitude

Figure 16: Object eccentricity 800 - 850 km altitude

The eccentricity plot confirms that these objects are in nearly circular orbits. A closer look at the inclination distribution shows clear congestion among inclinations close to 96°-100°.

Finally, it can be shown that most of the objects lie close to 830 km altitude and 100 degrees inclination. From this, the final target altitude and inclination parameters for the target are: 830 km altitude and 98° ± 2° inclination. The work shown above clearly highlights the optimal orbital elements of the first target object.

4.2.2 Aggregation Orbit

When choosing a final aggregation orbit location, altitudes to prioritize are ones with a lower spatial density of debris since minimizing the possibility of collisions between the aggregation satellite and other objects is desirable. Thus, the two main locations in LEO that stand out are between the 1000-1400 km and 1600-2000 km range.

In order to choose from these regions, further analysis was conducted to identify a more efficient orbit, from a mission budgeting standpoint. This was done by estimating rough delta-V amounts from the possible boosting transfer that the collection satellite would need to perform after gathering a piece of debris. A simple Hohmann transfer model was created, where both the initial and final orbits were assumed to be circular orbits. This assumption is validated by research into the near-zero average eccentricity of orbital debris around an 800 km altitude. The following equations to model the Hohmann transfer, where ΔV_{total} is the overall delta-V required for the transfer, $v_{T@r_{p,a}}$ is the velocity needed at either the periapsis or apoapsis of the elliptical transfer orbit and $v_{A,B}$ is the velocity within the circular orbit at either the starting point A or ending point B.

$$\Delta V_{total} = \left|v_{T@r_p} - v_A\right| + \left|v_B - v_{T@r_a}\right|$$

$$v_{T@r_{p,a}} = \sqrt{\mu\left(\frac{2}{r_{p,a}} - \frac{1}{a_T}\right)} \qquad v_{A,B} = \sqrt{\frac{\mu}{a_{A,B}}}$$

Both regions of interest were analyzed and produced the resulting delta-V requirements which were plotted against the final orbit altitude in the figure below.

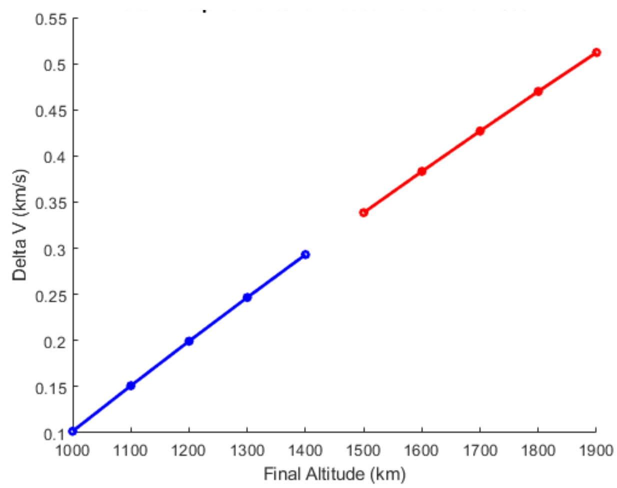

Figure 17: Delta-V requirements for boost transfer from 800 km

From this analysis, it is shown that the general delta-V requirement for the secondary potential aggregation region is about double that of the first region. The relationship between delta-V and final altitude is almost perfectly linear, but it is not immediately clear what altitude region would be best for aggregation from this, an additional analysis in transfer time was required. To do this, the following equation was used, calculating the transfer time from half of the orbital period using Kepler's Third Law.

$$T_{total} = \frac{1}{2}P_{total} = \pi\sqrt{\frac{{a_T}^3}{\mu}}$$

Transfer times were plotted vs possible final altitudes in both regions in the figure below.

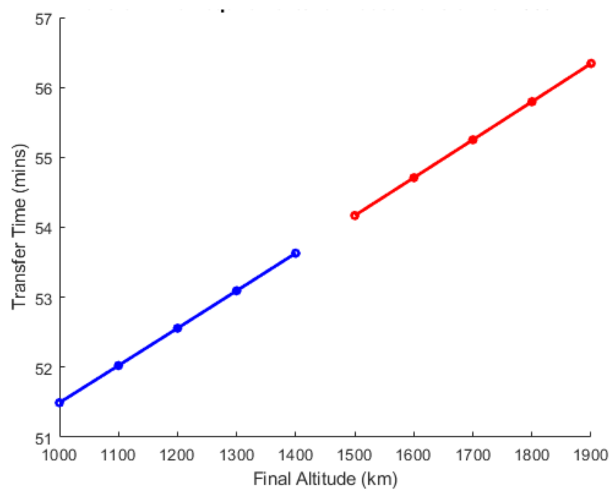

Figure 18: Transfer Time requirements for boost transfer from 800 km

The graph ended up looking visually similar to the delta-V graphs, but with lower slopes, indicating that transfer time is slightly less dependent on the final altitude. Looking at the transfer times, all are very close to only 1 hour for a simple boosting maneuver, which is incredibly quick. This gives validity to the mission's goal to be able to accomplish this maneuver a minimum of 20 times per year. However, the relative differences in time depending on altitude are pretty negligible, so solely the delta-V values will drive the final aggregation orbit location.

For this reason, the altitude chosen was one which had a lower delta-V requirement in order to allow a more efficient use of fuel for the collector satellite. The final aggregation orbit of 1200 km was chosen. This orbit is also in the middle of the first low spatial density range, protecting it from the possible drift of debris on the outskirts of the altitude range.

4.2.3 Tracking Algorithm

The initial analysis will focus on utilizing delta-v's to obtain the optimal debris targeting solution. Due to the nature of the mission design, it was determined that the Knapsack problem solution is the best implementation for the optimization of the targeting maneuvers. This is because the Knapsack problem can be solved by mixed integer linear programming, which can be easily implemented in Python for testing. The orienteering solution requires solvers that need additional licensing to be accessed. In addition, the Knapsack problem contains all necessary constraints, and it follows the original mission design, which aims to collect 1 object at a time and deposit it in the depot before returning to the collection orbit for another target. The integer knapsack problem was implemented due to the efficient utilization of the pyomo package.

To begin the analysis, delta-vs are calculated from the depot orbit (a 1300 km orbit) to all possible objects for capturing. There are two possible options to approach this: to calculate the delta-v towards all objects in the catalog, or to calculate the delta-v towards the "k nearest neighbors", which is calculated with a python optimization function. The k nearest neighbors' application allows for a faster computation time, as it gets rid of the objects that are extremely far away from the depot orbit by not calculating the delta-v towards them. The delta-v is calculated with a python script named "X4_DeltaV_vs_Distance.py". This script selects a target object, finds the k nearest neighbors, and loops through each pair of satellites to numerically compute the delta-V and angular momentum distances. The output of this script is a csv file containing all of the delta-v's from the particular node to a specified set of nodes (target objects).

Furthermore, the "OrbitToOrbit.py" script computes the delta-V based on the optimal phase free two-impulse orbit-to-orbit transfer. With numerical solvers that optimize computation time, this provides an alternative method to calculate delta-vs that can be implemented to improve the complexity of the solution. Like the previous solution, this script provides a csv file containing all the delta-vs from the depot to the debris target objects. A csv file containing all the delta-vs to solve the knapsack problem. A pork chop plot can be obtained from set delta-vs (as these are all phase-free transfers that are optimized for the best initial and final true anomalies).

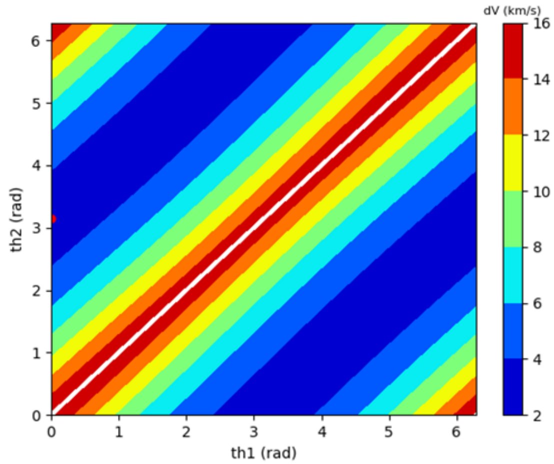

Figure 19: Example pork chop plot that can be computed for the optimal transfers between two orbits

With the resulting delta-vs, the Knapsack Problem can be implemented with the following steps: First, the depot is selected as the initial node. Then, the delta-V csv file for that node is loaded into the script, and the Satcat dataset from SPACETRACK is merged into the delta-V dataframe. A score is given to a particular object depending on RCS_SIZE (large, medium, small), and a budget is defined by the delta-v budget of the spacecraft and the time to complete the mission. Finally, the optimization solver is run, and the solution is obtained.

An example solution of the Knapsack Problem implementation is shown in Figure 20.

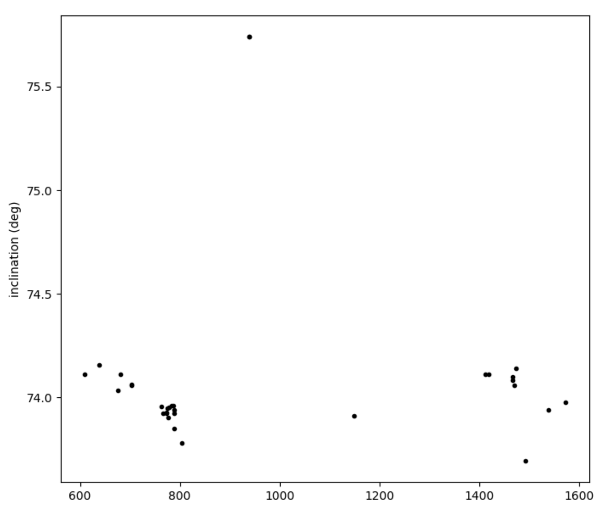

Figure 20: Example angular momentum vs position for target objects with Knapsack Problem solution

In conclusion, the Knapsack Problem Solution provides an innovative solution to the question of optimal target selection. The depot orbit can be selected as the initial node of the problem. Then, the optimal target to select that maximizes the score determined by physical characteristics of the target debris while also maximizing the use of the delta-v & time constraints can be determined.

4.3 Collection Satellite

4.3.1 Claw

As previously mentioned, the claw design is inspired by heritage missions that have utilized the same concept to perform dexterous tasks. The Canadarm 2, European Robotic Arm, and SMAP robotic arm have been researched in section 3 Literature Review. The claw consists of four arms and six degrees of freedom as shown below.

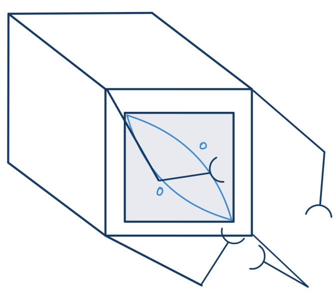

Figure 21: Satellite with claw & bag stored

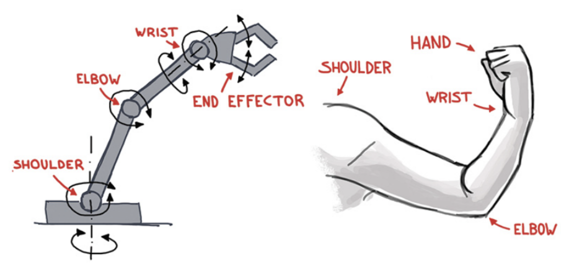

Figure 22: Six-degrees of freedom diagram[30]

Each arm is made of carbon fiber reinforced plastic and has six degrees of freedom. There is a shoulder, elbow, two degrees of freedom wrist and two hand components. To ensure that the orbital debris claw would be able to encapsulate a piece of debris that is 1 m^3 , the size of the claw was scaled down to be about 1.46 m.

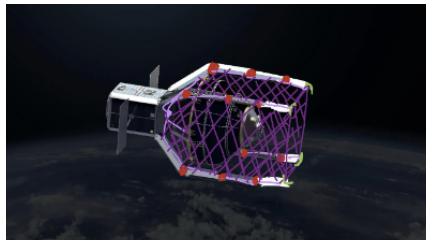

Figure 23: Inspiration of claw and net capture mechanism

4.3.2 Bag

To properly deploy the bag, the bag will be equipped with rings on opposite corners of the bag as well as the back of the bag as shown in the figures below.

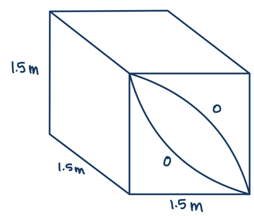

Figure 24: Sketch of expanded bag expanded

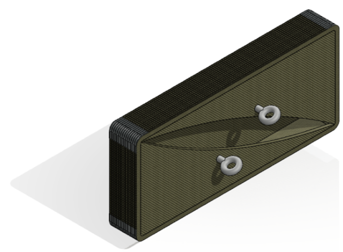

Figure 25: CAD of collapsed bag

The rings in the front of the bag are positioned in such locations so that the claw is able to clamp onto the rings and secure them when fully deployed. The ring in the back is used to keep the back end of the bag stationary and secure while the satellite is enroute to capture orbital space debris. Once the debris is captured, the front limbs of the robotic arm will fold inward and seal the bag shut. The servo motor will rotate the coil and release the back-end ring from the bag dispenser. The bag will then be transferred to the aggregator satellite by the robotic arms.

4.3.3 Dispenser

To be able to dispose of 20 pieces of debris, this mission will store and utilize 20 individual bags. Each bag will be dispensed using a coil and servomotor. The bag dispenser idea is inspired by a vending machine coil. The vending machine coil has items stored within the spacing of each coil and once the frontmost coil space is vacant, a motor rotates the entire coil and pushes the next item to the front-most coil space. This concept can be translated and applied to the orbital debris mission. An image is depicted below for better understanding and conceptualization:

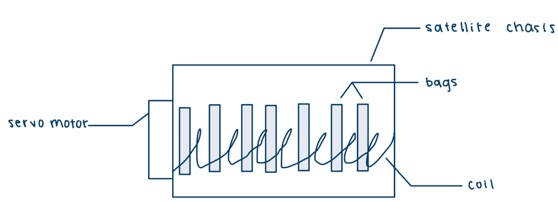

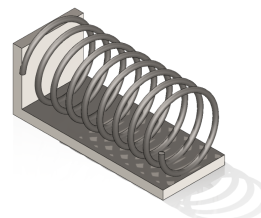

Figure 26: Sketch of bag dispenser **Figure 27**: CAD of dispenser

This mechanism would consist of a coil, back plate, and servo motor. The servo motor would rotate the coil and push the bags to the front and the back plate would be used to mount the servo motor onto the coil.

4.4 Aggregation Satellite

4.4.1 Bag Holding Mechanism

After choosing electropermanent magnets as the connection method between the bags and the aggregation satellite, initial power requirements for this mechanism were drafted.

The magnets chosen for this analysis were 50 mm 112 lb holding force electropermanent magnets from APW Company. These magnets take 12 V with a 0.86 A current, where they were modeled in a simple circuit where each magnet was a resistor of about 13.95 Ω. A circuit of 5 connected magnets were analyzed in both parallel and series. It was found for the parallel circuit, a supply voltage of 12 V would be needed, with a calculated current of 4.3 A. For the series circuit, a supply voltage of 60 V would be needed for the required 0.86 A current. The total power required was calculated using the following equation.

$$P = IV$$

The total required power in both cases to ‘turn on’ all 5 magnets was calculated to be 51.6 W. Due to the high required current for the parallel circuit, and the proven concept that these magnets continuously be powered ‘on’ and not have that affect the strength of the magnetic field, the decision was made to use the series circuit design for the aggregation satellite. The satellite would have four separate circuits of each 5 electropermanent magnets, so that only one circuit would need to be powered at a time during rendezvous operations, allowing the total power requirement for this system to remain at 51.6 W. The four separate circuits would need to be housed each within their own extremity on the satellite, driving the design for small satellite-compatible deployable booms.

4.4.2 Deployable Boom

The DCB system chosen consists of 2 separate spools that will each have 2 co-wrapped DCBs within them. There is a small wall on either side of the spools to help guide the booms as they deploy. Two of these spools will fit into the bottom of the 6U structure of the satellite and will be connected to two rotary motors above, which will activate the deployment.

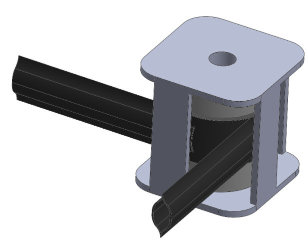

Figure 28: Single spool with 2 co-wrapped DCBs

4.4.3 Final Aggregation Satellite Design

The final design of the aggregation satellite will feature the two DCB spools, deployable solar arrays, and 4-units of available space to house all necessary components to fulfill function of the satellite. The 3D model of the 6U chassis is a modified version of the Removing Orbiting Aerosol Observatory (ROAO) CubeSat [31]. All other components were modeled by the team.

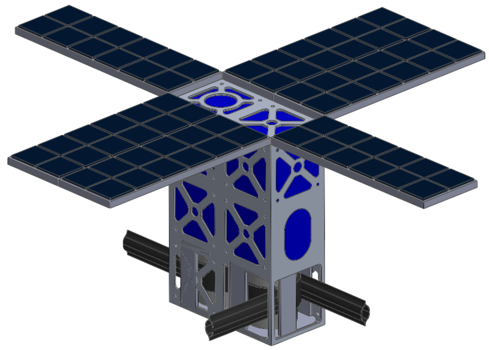

Figure 29: Aggregation satellite at start of boom deployment

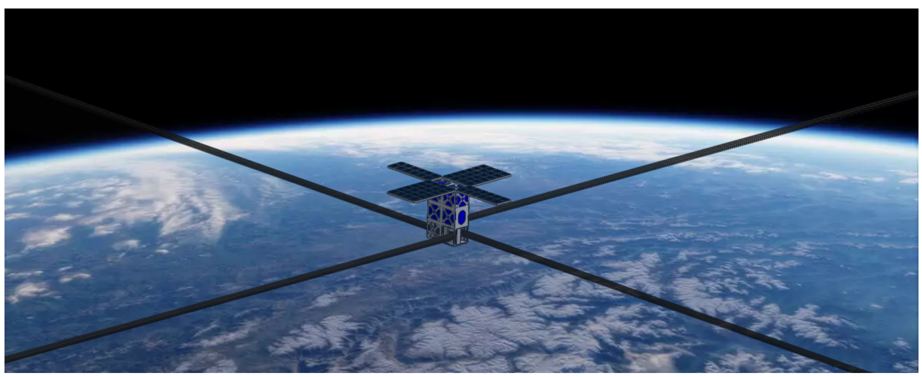

Figure 30: Aggregation satellite after boom deployment. Background Photo [32]

4.5 Propulsion

The initial propulsion system proposed was Electric Propulsion because it was believed to adhere closest to the problem statement's need for environmental sustainability. Although electric propulsion has "shown great potential in energy conservation and environmental protection," concerns were raised regarding its ability to provide the appropriate level of control necessary to carry out approaching maneuvers and intricate operations such as docking [33].

Please reference the Literature Review for the BHT-600 specifications and additional information. An additional mission requirement was defined and derived from a NASA publication from the AMES Research Center that states that SmallSats "are considered to be those with wet masses below 500 kg” [34]. Using the findings from the Literature Review and this new maximum wet mass requirement, two BHT-600 thrusters were implemented to the BROOM mission design through the MATLAB code provided in Figure 31.

```
clc
clear all;

% Spacecraft and thruster parameters
m_dry = 180; % kg, dry mass
Isp = 1495; % seconds, specific impulse
g0 = 9.81;

% Initial and final orbits
h_i = 850e3; % m, initial orbit altitude
h_f = 1350e3; % m, final orbit altitude
mu = 3.986e14; % m^3/s^2, Earth gravitational parameter

% Delta-v required for the Hohmann transfer
a_i = h_i + 6378e3; % m, initial orbit radius
a_f = h_f + 6378e3; % m, final orbit radius
v_i = sqrt(mu/a_i); % m/s, initial velocity
v_f = sqrt(mu/a_f); % m/s, final velocity
delta_v = abs(v_f - v_i); % m/s, delta-v required
delta_v_km = delta_v/1000 % km/s, delta-v required

%Propellant mass calculations
m_prop_cycle = exp(delta_v/(Isp * g0))*3 % kg, propellant mass required per aggregation cycle
m_wet = 500; % kg, max wet mass assumed to allow for max propellant
m_prop_total = m_wet - m_dry % kg, total on-board propellant mass available

%Mission calculations
total_cycles = m_prop_total/m_prop_cycle %total aggregation cycles propellant permits
cycles_per_year = total_cycles/5 %aggregation cycles propellant permits per year assuming a 5 year mission lifetime
delta_v_cycle = delta_v*3 %assuming an additional delta_v is required for proximity operations & other
total_delta_v = (delta_v_cycle*total_cycles)/(60*60) %s, total time of thruster operational time in mission lifetime
```

Figure 31: Propulsion MATLAB script

The analysis performed through the MATLAB code above provides various estimates. Assuming a Homann Transfer, the delta-V required to complete this transfer is ~0.24 km/s. A cycle is defined as a single occurrence of the Collector Satellite collecting a target, boosting, delivering the target to the Aggregator Satellite, and returning to its initial altitude. The amount of propellant necessary for a cycle is ~3 kg of Xenon with some margin. The total number of cycles the mission can complete. Based on the mission and propulsion system, the satellite can complete ~105 cycles before running out of fuel. In order to reduce the overall debris in space rather than purely mitigate the debris that will be created, an estimate of 20 pieces of debris of at least ~1 m^3 in size needs to be removed from orbit every year [35]. This means that ~21 cycles can be completed per year, proving that the propulsion system can support the ideal mission goal. Lastly, the analysis estimates a delta-V per cycle of ~733 m/s and a total mission delta-V of ~21 km/s. This is a preliminary analysis and does not account for many important factors such as drag, more realistic orbit transfers, fuel loss along the trajectory, etc. However, this is a good place to start for a more robust analysis.

4.6 Mass Budget

The minimum payload mass for the launch vehicle to be used for both satellites was found by calculating each satellite's mass budget and adding them together.

		CBE	Cont.	Allocated	
1.0 Payload					55.8
1.1 Payload		50.576	5.224	55.8	
1.1.2 Cloth	10.26				
1.1.3 Coil	10				
1.1.4 Servo Motor	0.78				
1.1.5 Arm	28.536				
1.1.6 Camera	1				
2.0 Spacecraft Bus (dry)					124.2
2.1 Propulsion		4.5	0.9	5.4	
2.2 ADCS		9.391304348	1.408695652	10.8	
2.3 Communications		3.272727273	0.327272727	3.6	
2.4 C&DH		8.181818182	0.818181818	9	
2.5 Power		32.86956522	4.930434783	37.8	
2.6 Structure		44.18181818	4.418181818	48.6	
2.7 Thermal Control System		3.130434783	0.469565217	3.6	
2.8 Other (ECLSS, etc.)		4.32	1.08	5.4	
3.0 Spacecraft Dry Mass (loaded mass - (consumables + propellant))					180
4.0 Consumables					0
5.0 Propellant					320
6.0 Loaded Mass					500
7.0 Kick Stage					0
7.1 Kick Stage Structure		--	--	0	
7.2 Kick Stage Propellant		--	--	0	
8.0 Injected Mass					500
9.0 Launch Vehicle Adapter					136
10.0 Boosted Mass					636
11.0 Margin					190.8
12.0 Collection Satellite Payload for Launch Vehicle					826.8 kg

Figure 32: Collection satellite mass budget

	CBE	Cont.	Allocated		
1.0 Payload					4.91959
1.1 Payload		2.2	2.71959	4.91959	
1.1.1 Boom	1.7				
1.1.2 Electropermanent Magnets	0.5				
2.0 Spacecraft Bus (dry)					7.07941
2.1 Propulsion		0	0	0	
2.2 ADCS		0.834713043	0.125206957	0.95992	
2.3 Communications		0.218163636	0.021816364	0.23998	
2.4 C&DH		0.545409091	0.054540909	0.59995	
2.5 Power		1.982443478	0.297366522	2.27981	
2.6 Structure		2.181636364	0.218163636	2.3998	
2.7 Thermal Control System		0.208678261	0.031301739	0.23998	
2.8 Other (ECLSS, etc.)		0.287976	0.071994	0.35997	
3.0 Spacecraft Dry Mass (loaded mass - (consumables + propellant))					11.999
4.0 Consumables					0
5.0 Propellant					0
6.0 Loaded Mass					11.999
7.0 Kick Stage					0
7.1 Kick Stage Structure		--	--	0	
7.2 Kick Stage Propellant		--	--	0	
8.0 Injected Mass					11.999
9.0 Launch Vehicle Adapter					4.5
10.0 Boosted Mass					16.499
11.0 Margin					7.071
12.0 Aggregation Satellite Payload for Launch Vehicle					23.57 kg

Figure 33: Aggregation Satellite mass budget

Payload for Launch Vehicle	
Collection Satellite	826.8
Aggregation Satellite	23.57
Total	850.37 kg

Figure 34: Total mass budget

The process for calculating the Collection Satellite's and the Aggregation Satellite's Payload for Launch Vehicle mass is the same and is found by using the SMAD.

5 Scale-Up of Design Approach

ADR missions can be profitable in several ways such as charging defunct satellite owners. This can be done through a fee-for-service model, similar to how waste management companies charge customers for removing their trash. Satellite owners of defunct satellites or debris are not penalized per se, but they are held responsible for the removal of their space objects under international space law. If they fail to do so, they may face legal consequences such as fines or denial of future launch licenses. Additionally, there may be reputational and financial costs associated with leaving debris in space.

Just like for defunct satellite owners, owners of operational satellites could be charged fees for the proposed satellites to remove debris for them. There are concentrated areas of debris that are of high interest for many uses. While avoidance maneuvers are constantly performed for spacecraft operating in high-density orbits to avoid debris, there is always a risk that debris will collide with your satellite. As a risk mitigation strategy, they could hire these services for a fee in order to reduce their mission risk.

Partnerships and grants are another way that would allow this mission design to be a realistic solution. Facilities such as the NASA Langley Research Center in Virginia are already facilitating the development of missions such as the ACS3 Satellite with the research of deployable booms. This shows that there are research facilities available that might be willing to partner with this mission, or fund development of components in some capacity.

6 Implications of Design Approach

The Concept of Operations described above is a novel idea with a novel design. No mission like this has ever been proposed before. The goal for most ADR missions is to deorbit and burn upon re-entry, and they also tend to target a single object rather than multiple ones. The end-of-life plan for this mission can help change the way ADR missions are thought of as it introduces a different plan for purpose that can be less wasteful. The proposed mission fits within the new area of circular space economies. Therefore, the mission has the potential to be highly profitable, something that is hard to do in the realm of space sustainability.

Appendix A: Contact Information

Team member: Aubrey L. Baker

Address: 10955 Brighton Ln Frisco, TX 75033

Email: aubreylane@me.com

Phone number: (623) 337 - 6013

Team member: Mauricio Martinez Elizondo

Address: 2035 Lima Loop Laredo, TX 78045

Email: mauriciome08@outlook.com

Phone Number: (956) 382-1084

Team member: Diana Segura Lerma

Address: 2093 Gus Moran El Paso, TX 79936

Email: dianasegura@utexas.edu

Phone Number: (915) 691-0586

Team member: Madison Vaughan

Address: 4420 Red River St. Austin, TX 78751

Email: vaughanmadi@utexas.edu

Phone Number: (281) 630-0527

Advisor: Adam Nokes

Address: 2617 Wichita St. Austin, TX 78712

Email: adamnokes@utexas.edu

Phone Number: (512) 364-1880

Appendix B: University and Program Description

The University of Texas at Austin is a leading research public university with a diverse set of undergraduate programs, and as the flagship school of the University of Texas, has produced many world-renowned alumni across the globe.

The Department of Aerospace and Engineering Mechanics (ASE/EM) offers interdisciplinary undergraduate and graduate programs for students. As one of the top 10 schools in the nation for the undergraduate and graduate aerospace engineering programs, as reported by *U.S. News & World Report*, the ASE/EM department emphasizes research and project-based learning in astronautics, space engineering, aviation, robotics, computational engineering, and theoretical and experimental mechanics. Students work closely with world-renowned faculty members to understand and evaluate the most recent challenges in modern aerospace engineering, and solve ever-pressing global and societal problems.

The ASE/EM Department is home to many multidisciplinary research laboratories, including labs which develop autonomous unmanned aerial vehicles, space-object visualization systems, modern satellite systems, and more. The culmination of the ASE/EM undergraduate program is displayed in the product of the students' work in their Senior Design courses. All work done for this proposal displays the learning, knowledge, and skill of exemplary engineering students from this program.

Appendix C: Industry Expert Description

The work presented in this mission design proposal could not have been possible without the help of various industry experts who provided their expertise and advice throughout the process. Ben Clark from Lockheed Martin SkunkWorks provided insightful advice to the team about developing a comprehensive Concept of Operations for the mission. He gave us guidance and mentoring at earlier stages of the project, when a lot of the ideas that ended up in our final design were still in question. Thanks to Ben's advice, the team was able to develop a well-rounded design that took into consideration factors such as economic potential and adaptability to different scenarios.

Dr. Scott Dorrington provided technical advice on the debris target selection algorithm. As a postdoctoral fellow at MIT's Space Enabled Group, he works on developing methods to ensure sustainable behavior in space through the Space Sustainability Rating framework. The work done for the debris target selection algorithm was inspired by previous collaboration between Mauricio, a member of the team, and Dr. Dorrington. His technical expertise on matters of mission optimization and orbital mechanics was extremely helpful to the developments of this mission.

Appendix D: Educational Experience

The SmallSat Alliance Collegiate Space Competition has proved to be a valuable educational experience for each of the students involved. I instruct the spacecraft capstone design courses at the University of Texas at Austin in the Aerospace Engineering and Engineering Mechanics department. Students complete a two semester sequence of courses that use team projects to instruct the Systems Engineering curriculum. Here is my evaluation of their educational experience during the past two semesters, based on the ABET Student Outcomes designated for this course. Each criterion is evaluated on the Likert 5 point scale that address the following question:

Did the students achieve the designated Student Outcome?

1. Strongly disagree
2. Disagree
3. Neither agree nor disagree
4. Agree
5. Strongly agree

Each ABET Student Outcome is evaluated according to this scale and a comment is provided below:

1) an ability to identify, formulate, and solve complex engineering problems by applying principles of engineering, science, and mathematics

Strongly agree. Orbital debris is a very complex problem and the team applied engineering principles to create a notional platform for debris removal that would be impactful and help reduce risk in the LEO environment.

2) an ability to apply engineering design to produce solutions that meet specified needs with consideration of public health, safety, and welfare, as well as global, cultural, social, environmental, and economic factors

Strongly agree. The team applied engineering design to produce solutions that met the needs of the project with consideration of the following factors: a) safe operation of orbital assets LEO is key to maintaining awareness of climate change and its impacts on public health; b) a proliferation of debris in LEO makes human orbital operations less safe and this project addresses that risk; c) orbital debris impacts the financial welfare of organizations that operate in LEO; d) global factors are addressed in discussion of the ownership of orbital debris as it relates to space law; e) social factors are addressed in the context of societal benefits to preventing further accumulation of orbital debris; f) environmental factors are addressed by this project in the form of a proposed method for cleaning up the space environment; g) economic factors are addressed by proposing a small satellite platform to aggregate debris that is much less expensive than previous methods of full size satellite debris removal.

3) an ability to communicate effectively with a range of audiences

Strongly agree. The team displayed excellent communication skills in written format, via this proposal, and in verbal format, via a series of four design reviews over the course of two semesters.

4) an ability to recognize ethical and professional responsibilities in engineering situations and make informed judgments, which must consider the impact of engineering solutions in global, economic, environmental, and societal contexts

Strongly agree. The team addressed environmental ethics in the text of the proposal and in design reviews for the capstone courses.

5) an ability to function effectively on a team whose members together provide leadership, create a collaborative and inclusive environment, establish goals, plan tasks, and meet objectives

Strongly agree. The team functioned very well and together they provided leadership. My observations were that the team environment was both collaborative and inclusive, and every team member made substantial contributions to the project.

6) an ability to acquire and apply new knowledge as needed, using appropriate learning strategies

Strongly agree. A great deal of new knowledge was required, and applied, in the areas of orbital debris taxonomy, ground and space based tracking, and space situational awareness.

Appendix E: References

[1] “A brief history of space debris: The Aerospace Corporation,” Aerospace Corporation, 02-Nov-2022. [Online]. Available: https://aerospace.org/article/brief-history-space-debris. [Accessed: 29-Mar-2023].

[2] V. L. Foreman, A. Siddiqi, and O. De Weck, “Large Satellite Constellation Orbital Debris Impacts: Case Studies of OneWeb and SpaceX Proposals,” AIAA SPACE and Astronautics Forum and Exposition. American Institute of Aeronautics and Astronautics, Sep. 12, 2017. doi: 10.2514/6.2017-5200.

[3] “Ares,” *NASA*. [Online]. Available: https://orbitaldebris.jsc.nasa.gov/quarterly-news/. [Accessed: 08-Mar-2023].

[4] C. Bonnal, D. McKnight, "Situation Report on Space Debris", International Academy of Astronautics, pp. 125-127, 2016.

[5] L. T. DeLuca, F. Bernelli, F. Maggi, P. Tadini, C. Pardini, L. Anselmo, M. Grassi, D. Pavarin, A. Francesconi, F. Branz, S. Chiesa, N. Viola, C. Bonnal, V. Trushlyakov, and I. Belokonov, “Active space debris removal by a hybrid propulsion module,” Acta Astronautica, vol. 91, pp. 20–33, 2013.

[6] Lorenzo Federici, Alessandro Zavoli, Guido Colasurdo, On the use of A* search for active debris removal mission planning, Journal of Space Safety Engineering, Volume 8, Issue 3, 2021, Pages 245-255, ISSN 2468-8967, https://doi.org/10.1016/j.jsse.2021.07.003.

[7] J. R. Wertz and W. J. Larson, Space mission analysis and design. Torrance, CA: Microcosm Press, 1999.

[8] “Science & Technology Book series,” NASA. [Online]. Available:
https://descanso.jpl.nasa.gov/SciTechBook/SciTechBook.html. [Accessed: 20-Apr-2023].
[9] S. Caldwell, “4.0 in-space propulsion,” NASA, 10-Oct-2021. [Online]. Available:
https://www.nasa.gov/smallsat-institute/sst-soa/in-space-propulsion#_Toc114987898. [Accessed: 20-Apr-2023].
[10] “High throughput 600 watt hall effect thruster for space exploration - NASA.” [Online]. Available:
https://ntrs.nasa.gov/api/citations/20170001303/downloads/20170001303.pdf?attachment=true. [Accessed: 20-Apr-2023].
[11] “Overview of Busek Electric Propulsion.” [Online]. Available:
http://electricrocket.org/2019/926.pdf. [Accessed: 20-Apr-2023].
[12] Axthelm, B. Klotz, I. Retat, U. Schlossstein, W. Tritsch, and S. Vahsen, “Net capture system for debris removal demonstration mission,” in 7th European Conference on Space Debris, ESOC, Darmstadt, Germany, 2017.
[13] “Removedebris,” *RemoveDEBRIS mission | University of Surrey*. [Online]. Available:
https://www.surrey.ac.uk/surrey-space-centre/missions/removedebris. [Accessed: 20-Mar-2023].
[14] European Space Agency (ESA), “ClearSpace-1: Earth's first Space Debris Removal Mission,” *SciTechDaily*, 01-Apr-2022. [Online]. Available:
https://scitechdaily.com/clearspace-1-earths-first-space-debris-removal-mission/. [Accessed: 07-Dec-2022].
[15] D. Clery, “Europe plans space claw to capture orbiting junk,” *Science*, 01-Dec-2020. [Online]. Available:

https://www.science.org/content/article/europe-plans-space-claw-capture-orbiting-junk. [Accessed: 07-Dec-2022].

[16] J. Reed and S. Barraclough, “Development of harpoon system for capturing space debris,” in 6th European Conference on Space Debris, vol. 723, p. 174, 2013.

[17] K. Atherton, “Satellite launches harpoon to catch debris in orbit,” *C4ISRNet*, 19-Aug-2022. [Online]. Available: https://www.c4isrnet.com/c2-comms/satellites/2019/02/15/satellite-launches-harpoon-to-catch-debris-in-orbit/. [Accessed: 29-Sep-2022].

[18] Canadian Space Agency, “Canadarm2's data sheet,” *Canadian Space Agency*, 08-May-2019. [Online]. Available: https://www.asc-csa.gc.ca/eng/iss/canadarm2/data-sheet.asp. [Accessed: 08-Apr-2023].

[19] “European robotic arm,” ESA. [Online]. Available: https://www.esa.int/Science_Exploration/Human_and_Robotic_Exploration/International_Space_Station/European_Robotic_Arm#:~:text=The%20robotic%20arm%20brings%20new,in%20real%20time%20or%20preprogrammed. [Accessed: 29-Mar-2023].

[20] “Toray_Space-Satellite-Launch_Advanced-Composite-Materials_Selector-Guide.pdf.” Toray Advanced Composites.

[21] H. Cruijssen, M. Ellenbroek, M. Henderson, H. Petersen, P. Verzijden, and M. Visser, “The european robotic arm: A high-performance mechanism finally on its way to space,” In the 42nd Aerospace Mechanism Symposium, 2014.

[22] “Vega-Users-Manual_ Issue-04_April-2014.pdf.” Ariane Space Service & Solutions.

[23] “Data 20Sheet 2048-F-1M.pdf.” CS Hyde Company, Lake Villa.

[24] "Beta cloth & beta fabric | dunmore aerospace," *Dunmore*. [Online]. Available: https://www.dunmore.com/products/beta-cloth.html. [Accessed: 20-Apr-2023].

[25] "stuff-toolkit-stronger-demo.pdf." WGBH Educational Foundation, 2010.

[26] K. Doyle and M. A. Peck, "Safe, failure-tolerant CubeSat docking using passive magnetic mechanisms," *55th AIAA Aerospace Sciences Meeting*, 2017.

[27] A. N. Knaian, Electropermanent magnetic connectors and actuators: devices and their application in programmable matter. PhD thesis, Massachusetts Institute of Technology, 2010.

[28] J. M. Fernandez, G. Rose, O. R. Stohlman, C. J. Younger, G. D. Dean, J. E. Warren, J. H. Kang, R. G. Bryant, and K. W. Wilkie, "An advanced composites-based solar sail system for interplanetary small satellite missions," *2018 AIAA Spacecraft Structures Conference*, 2018.

[29] W. K. Wilkie, "Overview of the NASA advanced composite solar sail system (ACS3) technology demonstration project," *AIAA Scitech 2021 Forum*, 2021.

[30] R. Caja Calleja, "An Arduino controlled robot arm," Servo Magazine. [Online]. Available: https://www.servomagazine.com/magazine/article/an-arduino-controlled-robot-arm. [Accessed: 29-Mar-2023].

[31] Interfluo, "Sat Chasis 2x3.SLDPRT." GrabCAD Community, 09-Oct-2021.

[32] S. Stanley, "Low Earth Orbit: Troposphere and Stratosphere," Wondrium Daily, 10-Aug-2020. [Online]. Available: https://www.wondriumdaily.com/low-earth-orbit-troposphere-and-stratosphere/. [Accessed: 29-Apr-2023].

[33] Y. Nie, W. Ouyang, Z. Zhang, G. Li, and R. Zheng, "Multi-parameter optimization analysis of hydrodynamic performance for RIM-driven thruster," MDPI, 12-Jan-2023. [Online]. Available: https://www.mdpi.com/1996-1073/16/2/891. [Accessed: 20-Apr-2023].

[34] “Small spacecraft overview - NASA technical reports server (NTRS).” [Online]. Available: https://ntrs.nasa.gov/api/citations/20190031730/downloads/20190031730.pdf. [Accessed: 20-Apr-2023].

[35] J.-C. Liou, N. L. Johnson, J.-C. Liou, and R. Walker, “A sensitivity study of the effectiveness of active debris removal in leo,” Acta Astronautica, 23-Aug-2008. [Online]. Available: https://www.sciencedirect.com/science/article/pii/S0094576508002634?casa_token=Poz1WcJ-yqcAAAAA%3AVVF6PwhijvK1ru1oazHi6VxTDu2CiWbvuZGnBTlFYObyAnmbZjBirYEIhzbXrCa_1911p78kmHRK. [Accessed: 20-Apr-2023].